Original Article

FUT10 is related to the poor prognosis and immune infiltration in clear cell renal cell carcinoma

Yuqi Zhang[#], Ke Cui[#], Rong Qiang, Lin Wang

Center of Medical Genetics, Northwest Women's and Children's Hospital, Xi'an, China

Contributions: (I) Conception and design: L Wang; (II) Administrative support: L Wang; (III) Provision of study materials or patients: Y Zhang, K Cui; (IV) Collection and assembly of data: Y Zhang, K Cui, R Qiang; (V) Data analysis and interpretation: Y Zhang, K Cui, R Qiang; (VI) Manuscript writing: All authors; (VII) Final approval of manuscript: All authors.

[#]These authors contributed equally to this work as co-first authors.

Correspondence to: Lin Wang, MM. Center of Medical Genetics, Northwest Women's and Children's Hospital, 1616 Yanxiang Road, Xi'an 710061, China. Email: wanglin_XA@163.com.

Background: Clear cell renal cell carcinoma (ccRCC), is highly metastatic with unfavorable oncologic outcomes. The metastatic dissemination and underlying mechanisms of ccRCC remain insufficiently understood. The expression of fucosyltransferases (FUTs) has been explored in multiple cancer types, which affect survival of tumor cells and oncology progress. However, the role of fucosyltransferase 10 (*FUT10*), a member of the FUT family, is still unclear in ccRCC. We aimed to investigate the effects of *FUT10* on the prognosis and immune infiltration of ccRCC via The Cancer Genome Atlas (TCGA) database.

Methods: The relationship between *FUT10* expression and clinical-pathologic features was evaluated by Welch's t-test, Wilcoxon signed-rank test, Dunn's test, and logistic regression based on TCGA datasets. The *FUT10* expression level was converted into a categorical variable by receiver operating characteristic (ROC) and the area under the curve (AUC). The factors associated with the prognosis were determined by Kaplan-Meier method. The function of *FUT10* was identified by functional enrichment analysis, gene set enrichment analysis (GSEA), gene correlation analysis, and immune infiltration analysis. At last, we verified the *FUT10* messenger RNA (mRNA) expression in ccRCC and adjacent kidney tissues by quantitative real-time polymerase chain reaction (qRT-PCR).

Results: Downregulated *FUT10* expression in ccRCC was associated with the clinical stage (P<0.001), T stage (P<0.001), M stage (P<0.001), and overall survival (OS) event (P<0.001). The ROC curve suggested that *FUT10* had a certain accuracy in the diagnostic ability in ccRCC (AUC =0.787). It was shown that patient survival was prolonged in the *FUT10* high-expression group. Meanwhile, multivariate analysis displayed that *FUT10* was an independent risk factor for ccRCC patients (P=0.003). Moreover, we uncovered that *FUT10* was involved in the phenotype of the immune response, oxidative phosphorylation (OXPHOS), arachidonic acid (AA) metabolism, and primary immunodeficiency (PID) by function enrichment analysis and GSEA. In addition, in the high *FUT10* expression group, natural killer (NK) CD56bright cells exhibited lower enrichment scores, and central memory T cells exhibited higher enrichment scores. Especially, *ARL8B*, a key factor in NK-mediated cytotoxicity, had a certain correlation with *FUT10* (r=0.590, P<0.001). Compared to the normal kidney tissues, the *FUT10* mRNA expression in the ccRCC was decreased (P=0.004).

Conclusions: *FUT10* might be a promising immune therapy target and prognostic biomarker in ccRCC.

Keywords: Fucosyltransferases (FUTs); fucosyltransferase 10 (*FUT10*); clear cell renal cell carcinoma (ccRCC); immune response; biomarker

Submitted Mar 19, 2024. Accepted for publication Nov 21, 2024. Published online Feb 26, 2025.
doi: 10.21037/tcr-24-449
View this article at: https://dx.doi.org/10.21037/tcr-24-449

Introduction

Renal cell carcinoma (RCC), a heterogeneous group of cancers derived from renal tubular epithelial cells, contributes to >90% of kidney neoplasm and is among the 10 most common cancers worldwide (1). Clear cell RCC (ccRCC), the predominant histology of RCC, is of over 5% incidence among all cancers, representing 75% of all cases of RCC and the majority of cancer-associated deaths (1,2). It has distinct immunological features and is characterized by high malignancy and insensitivity to chemotherapy or radiotherapy (3,4). Despite nephrectomy with curative intent, about 30% of ccRCC patients with localized disease eventually develop metastases (5,6). At present, the 5-year survival rate of localized ccRCC is 65%, but once metastasis occurs, it is reduced to 10–20% (7). Molecular-targeted drugs, tyrosine kinase inhibitors (TKIs), and immune checkpoint inhibitors (ICIs) have been increasingly recommended and investigated for ccRCC (8). In recent years, although the application of targeted therapy and immunotherapy have been extensively and successfully applied to ccRCC, a large number of patients have not responded to treatment due to immunological heterogeneity. There is still a long way to go for accurate ccRCC treatment. Therefore, it is critical to identify the specific molecular markers and therapeutic targets for the early diagnosis and treatment of ccRCC.

Highlight box

Key findings

- Fucosyltransferase 10 (*FUT10*) had extraordinary accuracy in the diagnosis and prediction the survival of clear cell renal cell carcinoma (ccRCC) patients. Besides, *FUT10* might participate in the development and progression of ccRCC through multi-signaling pathways and the impact the immune infiltrating cells, particularly central memory T and natural killer (NK) CD56bright cells.

What is known and what is new?

- Fucosyltransferases have been explored in multiple cancer types, which affect survival of tumor cells and oncology progress.
- High expression of *FUT10* was related to the prolonged survival of ccRCC. *FUT10* was involved in the phenotype of the immune response, and had a certain correlation with *ARL8B* (a key factor in NK cell-mediated cytotoxicity).

What is the implication, and what should change now?

- *FUT10* might be a promising immune therapy target and prognostic biomarker in ccRCC.

Aberrant glycosylation is not only considered a common aspect of cancer, but also often a hallmark of cancer (9,10). Fucosylation is a process in which fucose in guanosine diphosphate-fucose is transferred to its substrates (including N- and O-linked glycans in certain proteins, glycoproteins, or glycolipids) by fucosyltransferases (FUTs) in all mammalian cells (11). Recently, numerous studies have confirmed that increased fucosylation is a marker of malignant cell transformation and contributes to many abnormal events in the development and progression of cancer, such as uncontrolled cell proliferation, tumor cell invasion, cell-matrix interaction, angiogenesis, metastasis, immune escape, therapeutic resistance, and cancer cell signaling pathways (10-12). The main reason for altered glycosylation is the change in the expression of FUTs, which are the responsible enzymes for glycosylation. FUTs3-7 and FUTs9-11 have α-1,3-fucosyltransferase activity, whereas *FUT10* has been reported to be involved in a unique α1,3-fucosyltransferase activity with stringent substrate specificity, which is necessary to maintain stem cells in an undifferentiated state (13,14). However, *FUT10* in tumors has been rarely studied.

In this study, we investigated the expression, clinical-pathological features, immune infiltrates, and survival probability of *FUT10* in ccRCC patients using The Cancer Genome Atlas (TCGA) datasets. In addition, the biological function and mechanism of *FUT10* in ccRCC patients were investigated. Our results noted that *FUT10* was a potential prognostic biomarker and target for immune treatment of ccRCC. We present this article in accordance with the TRIPOD reporting checklist (available at https://tcr.amegroups.com/article/view/10.21037/tcr-24-449/rc).

Methods

Gene expression and clinical characteristics in TCGA

To investigate the expression pattern of *FUT10* on ccRCC, TCGA kidney renal cell carcinoma (KIRC) L3 high-throughput sequencing (HTSeq)-fragments per kilobase per million (FPKM) RNA sequencing (RNA-seq) data format was obtained from TCGA (https://portal.gdc.cancer.gov/; accessed on 12 March 2022). Then, it was converted to transcripts per million (TPM) formats for further analysis. RNA-seq data in TPM format were also obtained from TCGA and Genotype-Tissue Expression (GTEx) databases and processed by UCSC Xena's Toil process (https://xenabrowser.net/datapages/; accessed on

12 March 2022) (15). The $\log_2$(TPM +1) transformed expression data were applied for the heatmap and box plots to compare the messenger RNA (mRNA) expression of *FUT10* between different groups. Moreover, we used GSE126964 (7) datasets from the Gene Expression Omnibus (GEO) database to further testify the expression of *FUT10* in ccRCC. In addition, the mRNA expression level of *FUT10* was analyzed via the University of Alabama at Birmingham Cancer Data Analysis Portal (UALCAN) website. The Human Protein Atlas (HPA) website was used to acquire the expression of *FUT10* protein in ccRCC. All procedures performed in this study were in accordance with the Declaration of Helsinki (as revised in 2013).

Function enrichment and gene set enrichment analysis (GSEA) for FUT10

We analyzed the correlations between *FUT10* and differential genes by the DESeq2 package of R (v.3.6.3) (7). Then, Gene Ontology (GO) and GSEA were performed to investigate possible pathways by the ClusterProfiler package in R (16). Adjusted P<0.05 and false discovery rate (FDR) <0.25 were considered significant enrichment. The gene set database was from MSigDB Collections (https://www.gsea-msigdb.org/gsea/index.jsp), and the reference gene collection was C2.CP.V7.2.symbols.fmt (Curated).

Co-expression genes analysis

We used R to excavate genes that correlated with *FUT10* and then used the threshold |Cor| >0.69 and P<0.05 for heatmap analysis. The Ensembl 101 library was used to annotate the molecular ID (http://ftp.ensembl.org/pub/release-101/gtf/homo_sapiens/).

Immunocyte infiltration analysis

The relationship of *FUT10* and 24 types of immune cells was detected by single sample GSEA (ssGSEA) using the gene set variation analysis (GSVA) package and the data of normal groups were filtered out (17,18). The whole correlation analysis adopted the Spearman method.

Quantitative real-time polymerase chain reaction (qRT-PCR)

Adjacent kidney (n=10) and ccRCC tissue (n=13) were purchased from Shanghai Outdo Biotech Company, Shanghai, China. According to the manufacturer's instructions, total RNA was extracted using TRIzol reagent (Takara, Shiga, Japan), complementary DNA (cDNA) was synthesized, and the qRT-PCR was conducted and measured using $2^{-\Delta\Delta Ct}$ methods. Related primers were displayed as follows: *FUT10*: 5'-CAGCCAGCGTGTGAGAAA-3' (forward); 5'-TCCAAGACCAGCCCAATC-3' (reverse); β-actin: 5'-GAAGAGCTACGAGCTGCCTGA-3' (forward); 5'-CAGACAGCACTGTGTTGGCG-3' (reverse).

Statistical analysis

The R program (R Foundation for Statstical Computing, Vienna, Austria) was used to conduct all statistical analyses. We analyzed the expression of *FUT10* in ccRCC from the TCGA database using Welch's *t*-test, Wilcoxon signed-rank test, and Dunn's test. The receiver operating characteristic (ROC) curve was generated using the pROC package. Kaplan-Meier analysis and multivariate Cox analysis were viewed using the survival package. P<0.05 was considered significantly different.

Results

Downregulated expression levels of FUT10 in patients with ccRCC

The gene expression data and clinical data of 539 primary tumors and 72 normal samples were downloaded from the TCGA database, including patients' gender, age, histological grade, pathologic stage, tumor, node, metastasis (TNM) stage, and survival data. Based on the medium levels of *FUT10*, we divided them into high or low groups. Unpaired sample analysis showed that mRNA expression levels of *FUT10* in ccRCC tissues were significantly lower than those in adjacent tissues (*Figure 1A,1B*). GSE126964 also showed that *FUT10* was lowly expressed in tumor groups (*Figure 1C*; P<0.001). Moreover, the result of the paired sample analysis was consistent with the result of the unpaired sample analysis (*Figure 1D*; P<0.001). We also confirmed that the *FUT10* expression level was significantly decreased in the tumor tissue of ccRCC via the UALCAN website (*Figure 1E*). In addition, according to the results of the HPA database, the expression level of *FUT10* protein in normal tissue was significantly higher than that in tumor tissue (*Figure 1F*). These results verified the downregulated expression levels of *FUT10* in patients with ccRCC.

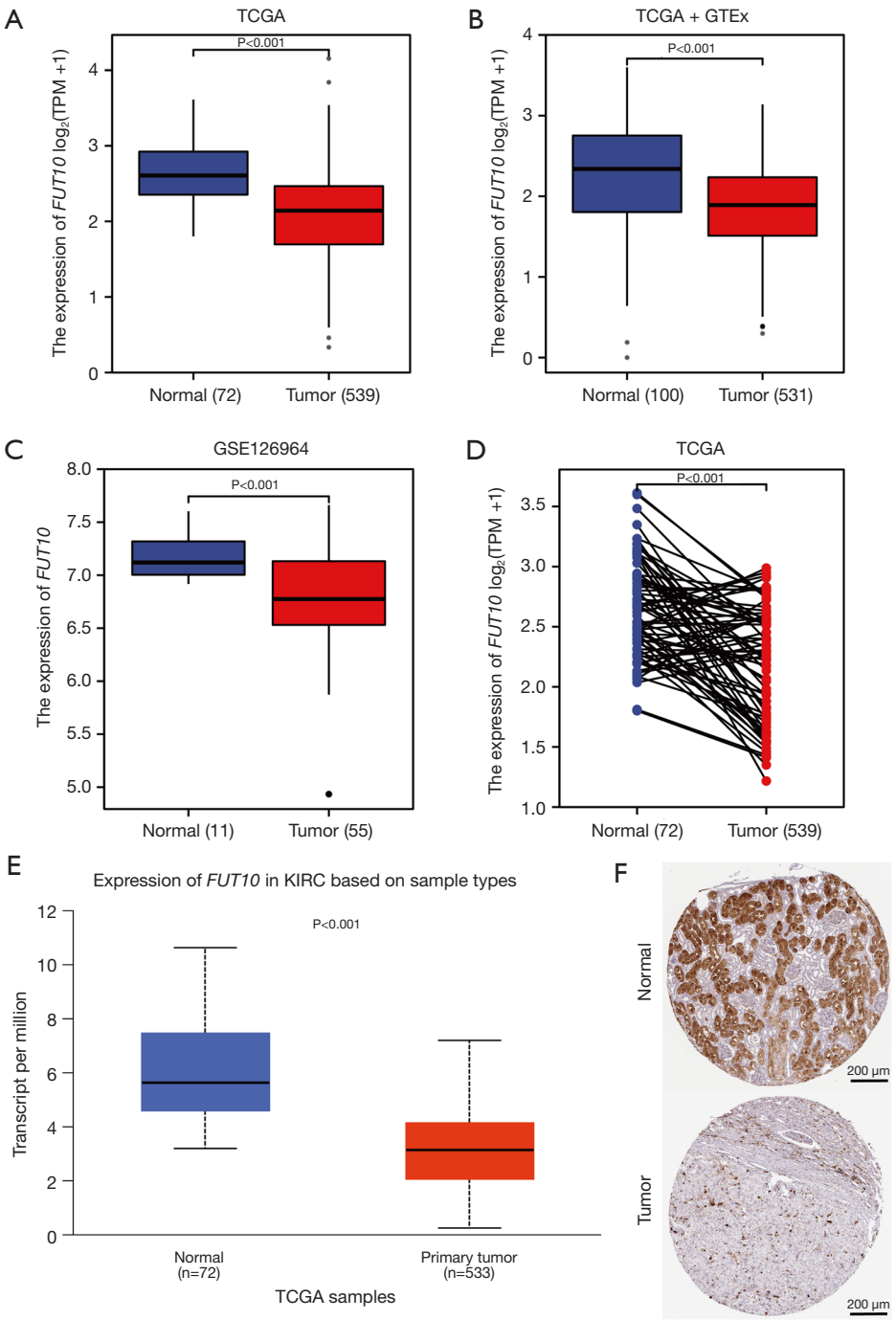

Figure 1 *FUT10* mRNA expression in ccRCC patients. (A) *FUT10* mRNA expression in ccRCC tissues and unpaired normal tissues of TCGA. (B) *FUT10* mRNA expression in ccRCC tissues of TCGA and normal tissues of GTEx combined with TCGA. (C) *FUT10* mRNA expression in ccRCC tissues and normal tissues based on the GSE126964 dataset. (D) *FUT10* mRNA expression in ccRCC tissues and paired adjacent tissues of TCGA. (E) *FUT10* mRNA expression in ccRCC tissues and adjacent tissues based on the UALCAN website. (F) *FUT10* protein expression in ccRCC tissues and adjacent tissues based on the HPA website (https://www.proteinatlas.org/ENSG00000172728-*FUT10*) (immunohistochemical staining). *FUT10*, fucosyltransferase 10; TPM, transcripts per million; TCGA, The Cancer Genome Atlas; GTEx, Genotype-Tissue Expression; KIRC, kidney renal cell carcinoma; mRNA, messenger RNA; ccRCC, clear cell renal cell carcinoma; UALCAN, University of Alabama at Birmingham Cancer Data Analysis Portal; HPA, Human Protein Atlas.

Table 1 The relationship between *FUT10* mRNA expression and clinical parameters of patients with ccRCC (n=539)

Characteristics	Low expression of *FUT10* (n=269)	High expression of *FUT10* (n=270)	P value
T stage			<0.001*
T1	110 (20.4)	168 (31.2)	
T2	41 (7.6)	30 (5.6)	
T3	112 (20.8)	67 (12.4)	
T4	6 (1.1)	5 (0.9)	
N stage (n=257)			0.39
N0	120 (46.7)	121 (47.1)	
N1	9 (3.5)	7 (2.7)	
M stage (n=506)			0.01*
M0	201 (39.7)	227 (44.9)	
M1	49 (9.7)	29 (5.7)	
Pathologic stage			<0.001*
Stage I	108 (20.0)	164 (30.6)	
Stage II	31 (5.8)	28 (5.2)	
Stage III	78 (14.5)	45 (8.3)	
Stage IV	50 (9.3)	32 (5.9)	
OS event			<0.001*
Alive	158 (29.3)	208 (38.6)	
Dead	111 (20.6)	62 (11.5)	
DSS event (n=528)			<0.001*
Alive	188 (35.6)	232 (43.9)	
Dead	74 (14.0)	34 (6.4)	
PFI event			<0.001*
Alive	166 (30.8)	212 (39.3)	
Dead	103 (19.1)	58 (10.8)	
Age (years)	62 [53, 70]	60 [51, 69]	0.07

Data are presented as n (%) or median [IQR]. *, P<0.05. *FUT10*, fucosyltransferase 10; mRNA, messenger RNA; ccRCC, clear cell renal cell carcinoma; OS, overall survival; DSS, disease-specific survival; PFI, progression-free interval; IQR, interquartile range.

Relationships between clinical pathological characteristics of patients with ccRCC and FUT10 mRNA level

As shown in *Table 1* and *Figure 2*, lower expression levels of *FUT10* were associated with histological grade (P<0.001), pathologic stage (P<0.001), T stage (P<0.001), M stage (P=0.01), overall survival (OS) (P<0.001), disease-specific survival (DSS) (P<0.001), and progression-free interval (PFI) (P<0.001), respectively. Other clinicopathological features, including gender (P=0.28), age (P=0.07), and N stage P=0.39), were not statistically significant.

Diagnostic value of FUT10 mRNA expression in ccRCC

The value for *FUT10* to distinguish ccRCC samples from normal samples was assessed by ROC curve analysis. The results showed a diagnostic value with an area under the curve (AUC) of 0.787 for *FUT10* [*Figure 3A*; 95% confidence interval (CI): 0.738–0.836]. When the cut-off value was 2.364, the sensitivity, specificity, and accuracy of *FUT10* were 75%, 67.3%, and 68.5%, respectively. The positive predictive value was 23.5% and the negative predictive value was 95.3%, indicating that *FUT10* was

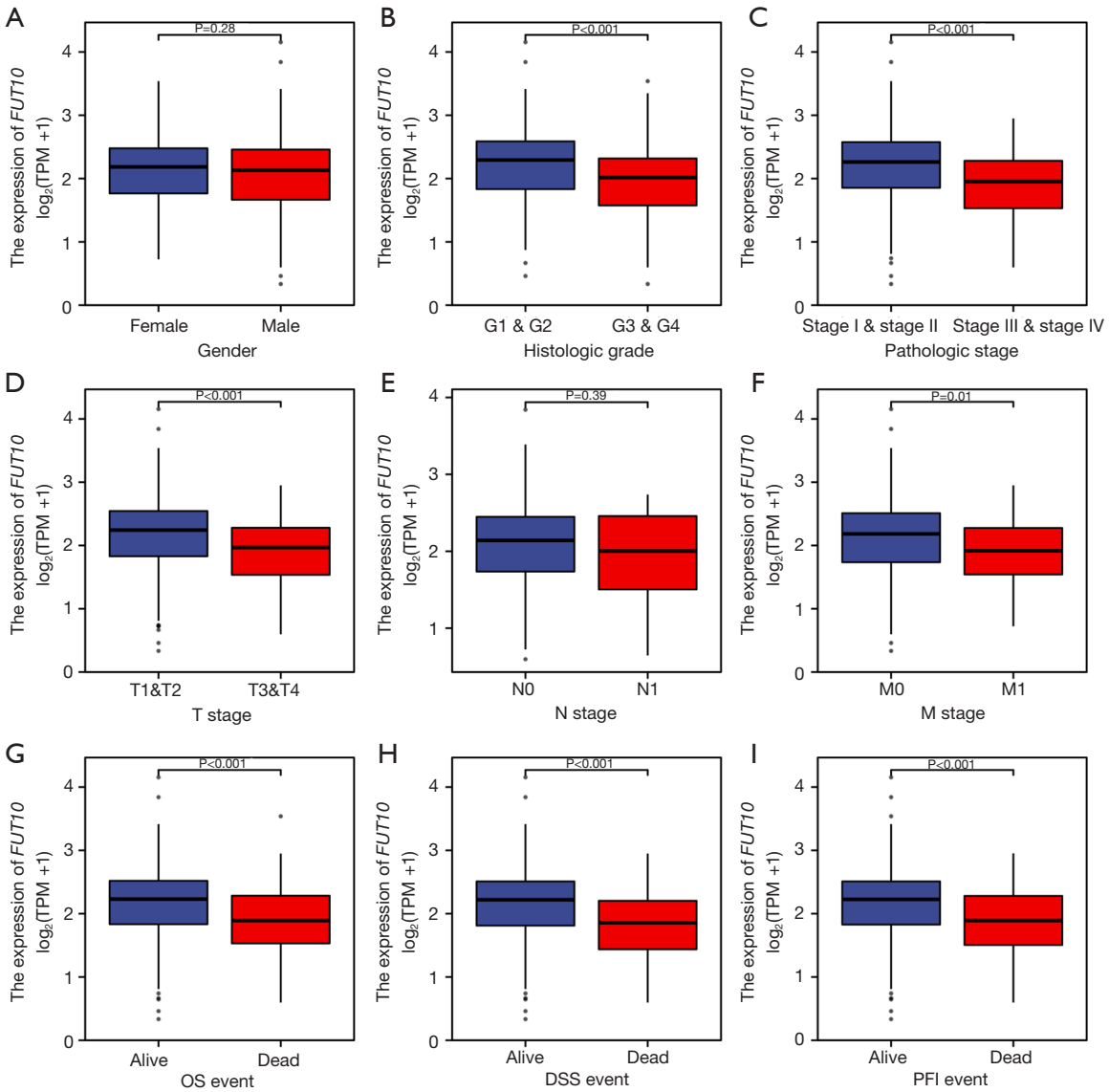

Figure 2 Correlation between expression of *FUT10* and clinicopathological parameters according to TCGA data analysis. (A) Gender. (B) Histologic grade. (C) Pathologic stage. (D) T classification. (E) N classification. (F) M classification. (G) OS event. (H) DSS event. (I) PFI event. *FUT10*, fucosyltransferase 10; TPM, transcripts per million; OS, overall survival; DSS, disease-specific survival; PFI, progression-free interval; TCGA, The Cancer Genome Atlas.

accurate in distinguishing ccRCC tissues from normal tissues.

FUT10 mRNA expression is an independent risk factor for survival in patients with ccRCC

According to the median expression of *FUT10*, Kaplan-Meier analysis exhibited that lower *FUT10* expression had a much worse OS, DSS, and progression-free survival (PFS) than those in high-*FUT10* groups (*Figure 3B-3D*; P<0.001). The univariate analysis showed that higher *FUT10* mRNA expression, pathological stage, and TNM stage were related to OS (*Table 2*). Moreover, multivariate analysis was revealed that *FUT10* was an independent prognostic variable of OS in ccRCC (*Table 2*; P=0.003). From the nomogram chart, we can see that the lower the *FUT10* expression, the less the

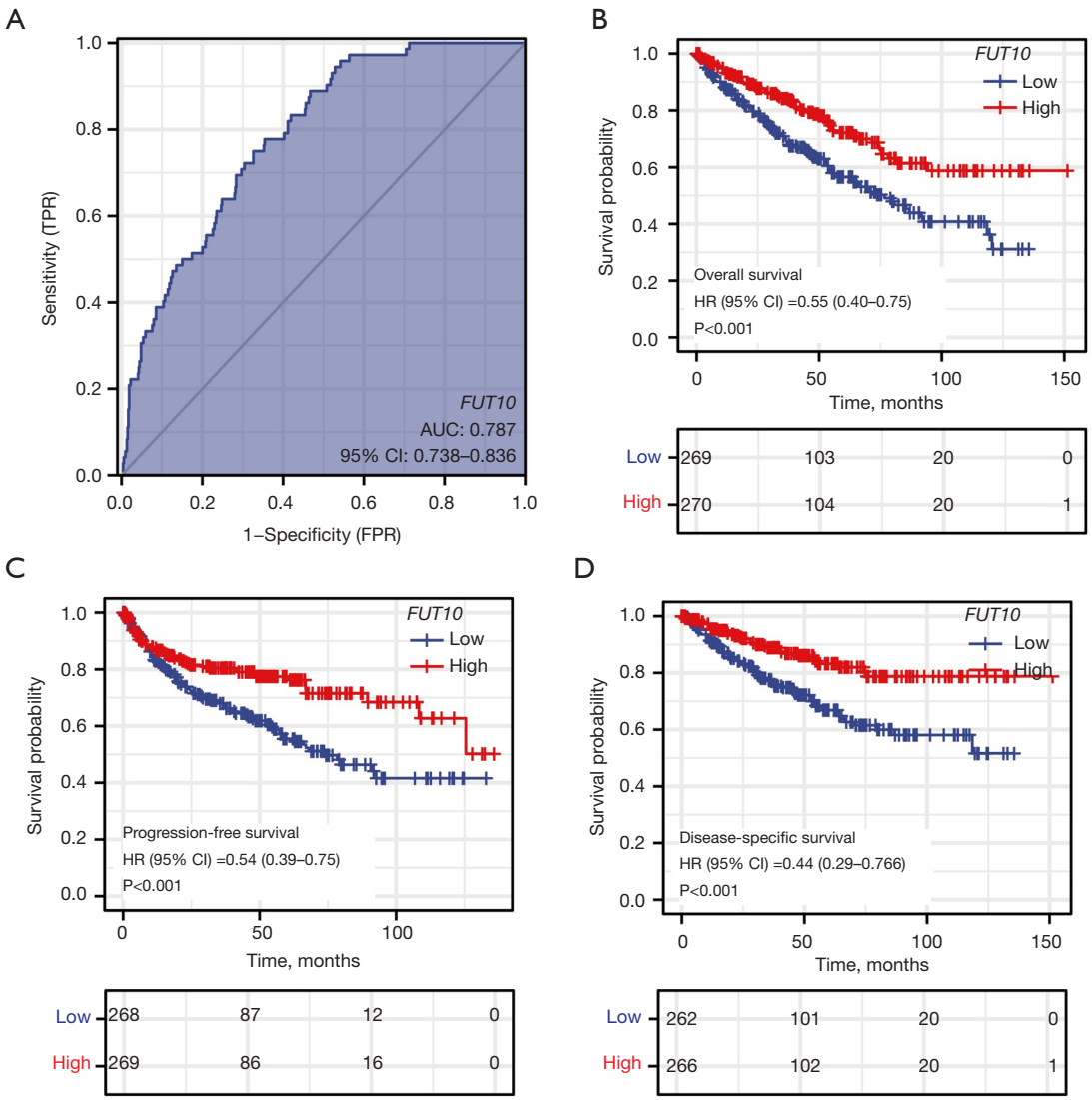

Figure 3 ROC curve and Kaplan-Meier analysis with *FUT10* mRNA expression according to TCGA data analysis. (A) ROC curve of *FUT10* mRNA expression in normal and tumor. (B) Kaplan-Meier analysis of OS in patients with ccRCC. (C) Kaplan-Meier analysis of PFS in patients with ccRCC. (D) Kaplan-Meier analysis of DSS in patients with ccRCC. TPR, true positive rate; FPR, false positive rate; *FUT10*, fucosyltransferase 10; AUC, area under the curve; CI, confidence interval; HR, hazard ratio; ROC, receiver operating characteristic; mRNA, messenger RNA; TCGA, The Cancer Genome Atlas; OS, overall survival; ccRCC, clear cell renal cell carcinoma; PFS, progression-free survival; DSS, disease-specific survival.

probability of survival for 1, 3, and 5 years (*Figure 4*).

Functional enrichment and GSEA dug FUT10-related mechanism

We conducted GO and Kyoto Encyclopedia of Genes and Genomes (KEGG) analyses to construct functional annotations. As shown in *Table 3* and *Figure 5A*, changes in the biological process of *FUT10* were correlated with acute inflammatory response, epidermis development, epidermal cell differentiation, humoral immune response, regulation of immune effector process, lymphocyte-mediated immunity, and so on. Moreover, we identified the signaling pathways that played important roles in ccRCC by

Table 2 Univariate and multivariate analysis of clinical factors on ccRCC patients with OS

Characteristics	Total, n	Univariate analysis		Multivariate analysis	
		Hazard ratio (95% CI)	P value	Hazard ratio (95% CI)	P value
Pathologic stage (III & IV *vs.* I & II)	536	3.946 (2.872–5.423)	<0.001*	1.109 (0.436–2.825)	0.83
T stage (T3 & T4 *vs.* T1 & T2)	539	3.228 (2.382–4.374)	<0.001*	2.080 (0.922–4.694)	0.08
N stage (N1 *vs.* N0)	257	3.453 (1.832–6.508)	<0.001*	1.882 (0.970–3.651)	0.06
M stage (M1 *vs.* M0)	506	4.389 (3.212–5.999)	<0.001*	2.734 (1.631–4.582)	<0.001*
FUT10 (high *vs.* low)	539	0.546 (0.400–0.745)	<0.001*	0.522 (0.339–0.806)	0.003*

*, P<0.05. ccRCC, clear cell renal cell carcinoma; OS, overall survival; CI, confidence interval; *FUT10*, fucosyltransferase 10.

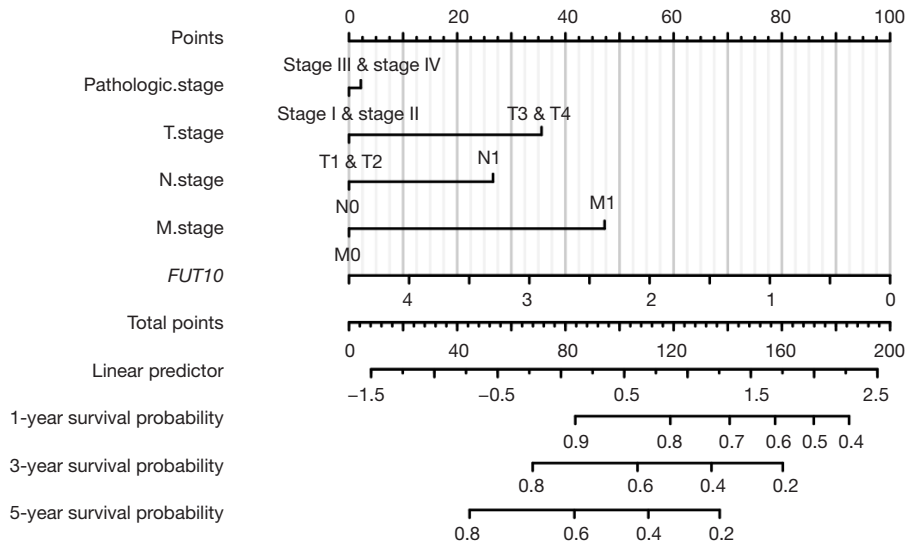

Figure 4 Prediction model of nomogram construction according to the results of TCGA data analysis. *FUT10*, fucosyltransferase 10; TCGA, The Cancer Genome Atlas.

GSEA. *Figure 5B-5D* shows that oxidative phosphorylation (OXPHOS), arachidonic acid (AA) metabolism, and primary immunodeficiency (PID) pathways were significantly enriched in the negative correlation with *FUT10* mRNA expression phenotype.

Analysis of co-expression genes

It has been shown that *ARL8B*, *STAM2*, *APPL1*, *ERLIN2*, *ANKFY1*, and *BAG4* play roles in tumor cell proliferation, migration, adhesion, cell cycle and survival, and immune response. Thus, to examine possible mechanisms of *FUT10* expression that affect ccRCC, the correlation of *FUT10* with these molecules was analyzed (*Figure 6A-6G*). The results showed that *FUT10* was positively associated with *STAM2*, *APPL1*, *ERLIN2*, *ANKFY1*, *BAG4*, and so on, which can influence tumor progression in multiple aspects, including cell proliferation, migration, cell cycle, and survival. The value of *ARL8B* was 0.590, which was related to natural killer (NK)-mediated cytotoxicity and was also listed in our results.

The relationship of FUT10 expression with immune infiltration

The relationship of *FUT10* expression with 24 different immunocytes was analyzed by ssGSEA with Spearman correlation analysis. It was shown that higher *FUT10*

Table 3 GO terms enriched in high- and low-*FUT10* groups by using GSEA

Ontology	ID	Description	Gene ratio	Bg ratio	P value	P adjusted	Q value
BP	GO:0002526	Acute inflammatory response	31/303	220/18,670	<0.001	<0.001	<0.001
BP	GO:0072376	Protein activation cascade	23/303	198/18,670	<0.001	<0.001	<0.001
BP	GO:0006958	Complement activation, classical pathway	19/303	137/18,670	<0.001	<0.001	<0.001
BP	GO:0002455	Humoral immune response mediated by circulating immunoglobulin	19/303	150/18,670	<0.001	<0.001	<0.001
BP	GO:0006959	Humoral immune response	28/303	356/18,670	<0.001	<0.001	<0.001
BP	GO:0009913	Epidermal cell differentiation	28/303	358/18,670	<0.001	<0.001	<0.001
BP	GO:0008544	Epidermis development	30/303	464/18,670	<0.001	<0.001	<0.001
BP	GO:0016064	Immunoglobulin mediated immune response	19/303	218/18,670	<0.001	<0.001	<0.001
BP	GO:0016485	Protein processing	22/303	328/18,670	<0.001	<0.001	<0.001
BP	GO:0051604	Protein maturation	22/303	397/18670	<0.001	<0.001	<0.001
BP	GO:0002449	Lymphocyte mediated immunity	20/303	352/18,670	<0.001	<0.001	<0.001
BP	GO:0050727	Regulation of inflammatory response	23/303	485/18,670	<0.001	<0.001	<0.001
BP	GO:0002697	Regulation of immune effector process	22/303	458/18,670	<0.001	<0.001	<0.001

GO, Gene Ontology; *FUT10*, fucosyltransferase 10; GSEA, gene set enrichment analysis; BP, biological process.

expression was positively related to central memory T (Tcm) cells and negatively associated with cytotoxic cells and NK CD56bright cells (P<0.001; *Figure 7A-7C*). Moreover, in higher *FUT10* expression groups, NK CD56bright cells showed lower enrichment scores, but the enrichment scores of Tcm were higher (*Figure 7D,7E*).

The verification of FUT10 expression in ccRCC tissues

We used qRT-PCR to verify the expression of *FUT10* mRNA in ccRCC tissues, and observed that *FUT10* mRNA was down-regulated in ccRCC tumors (n=10) compared with normal renal tissues (*Figure 8*; P=0.004).

Discussion

Glycosylation is one of the important post-translational modifications, which is regulated by the role glycosyltransferases (GTs) and glycosidases in glycoproteins and/or lipids. Abnormal glycosylation is not only a result of cancer, but also a driver of malignant phenotypes. Numerous findings have shown that the altered glycosylation of tumor cell proteins directly affects the growth, differentiation, transformation, adhesion, metastasis, and immune surveillance. At the same time, abnormal glycoproteins play an important role in the malignant transition and migration of tumors (19,20). FUTs can be used to identify tumors with well-differentiated cells and also could be used as a marker for early tumorigenesis (21,22). *FUT10* is located in Golgi apparatus, endoplasmic reticulum, and nucleoplasm, and has α-1,3-fucosyltransferase activity. *FUT10* is predicted to act upstream of or inside the cerebral cortex to maintain directed cell migration and the function of neural stem cell populations (23). However, there is limited maintenance research on the function of *FUT10* in tumors.

RCC is a malignant tumor characterized by energy metabolism reprogramming (24-27). In particular, the metabolic flux through glycolysis is partitioned (28-30), mitochondrial bioenergetics, OXPHOS, and lipid metabolism are impaired (28,31-34). In this scenario, to examine possible mechanisms of *FUT10* expression affecting ccRCC, FUTs are important regulators of the metabolic activity of mucins (such as *MUC1*) in ccRCC (33-35). In our study, we used TCGA and GEO databases to analyze the relationship between *FUT10* and the prognosis of ccRCC patients. We found that *FUT10* was lowly expressed in ccRCC tumors compared with normal kidney tissues, particularly in the later clinical stages III and IV. The results of logistic regression analysis suggested that *FUT10* was related to T stage, M stage, and pathological stage. Moreover, decreased *FUT10* expression was linked to poor OS, DSS, and PFI, showing a moderate ability for tumor

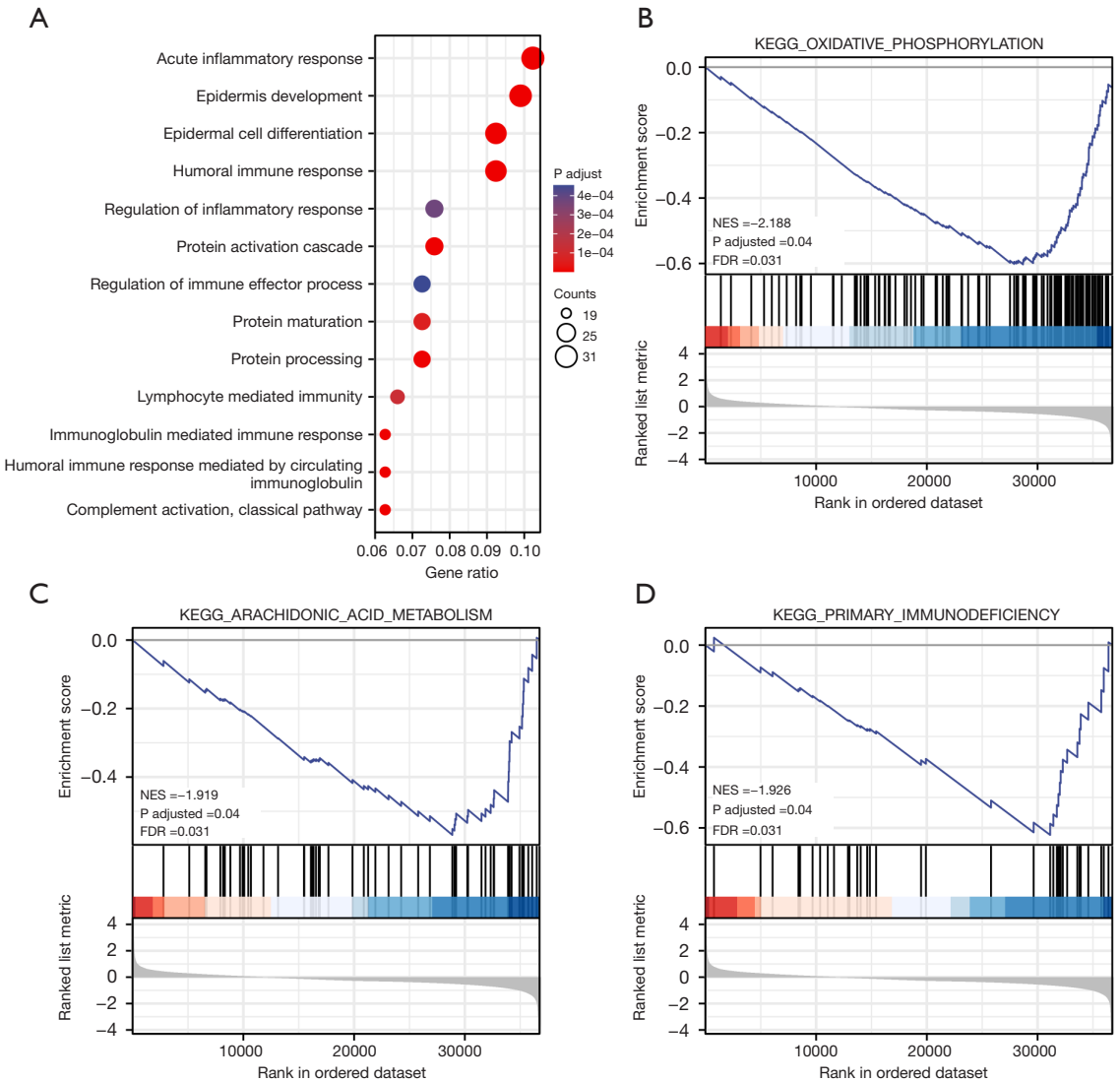

Figure 5 GO and KEGG were used to construct functional annotations based on TCGA data. (A) The biological function of *FUT10* was plotted. (B-D) OXPHOS, AA metabolism, and PID pathways were differentially enriched in the negatively correlated with *FUT10* expression. KEGG, Kyoto Encyclopedia of Genes and Genomes; NES, normalized enrichment score; FDR, false discovery rate; GO, Gene Ontology; TCGA, The Cancer Genome Atlas; *FUT10*, fucosyltransferase 10; AA, arachidonic acid; OXPHOS, oxidative phosphorylation; PID, primary immunodeficiency.

diagnosis and prediction. Besides, the Cox regression analysis showed that *FUT10* was an independent prognostic variable in ccRCC. The nomogram based on *FUT10* suggested that the lower the expression of *FUT10*, the lower the survival probability of patients, and showed a downward trend year by year. Overall, these findings revealed that *FUT10* might be a protective molecular and prognostic factor.

Regarding functional studies, we found that *FUT10* has significantly negative correlations with OXPHOS, AA metabolism, and PID pathways. Firstly, OXPHOS, mitochondrial adenosine triphosphate (ATP) generation coupled to oxygen consumption, is widely recognized as upregulated in tumors and associated with malignancies and tumor cell expansion (36). Currently, more and more chemotherapies aim at directly or indirectly suppressing OXPHOS levels in various tumors, such as triple-negative

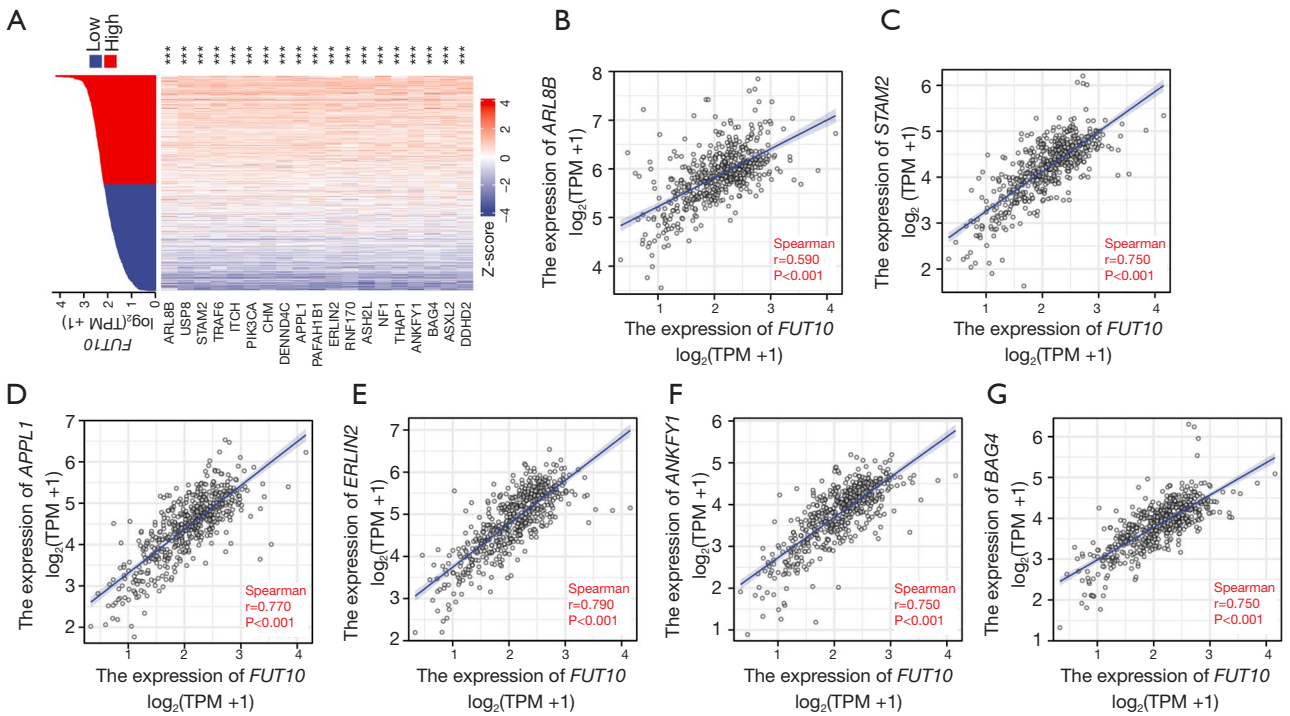

Figure 6 Analysis of possible correlation genes with *FUT10* expression in ccRCC from TCGA database. (A) The heat map exhibited *FUT10* possible correlation molecules. (B-G) *FUT10* was positively associated with *ARL8B*, *STAM2*, *APPL1*, *ERLIN2*, *ANKFY1*, and *BAG4*. ***, P<0.001. *FUT10*, fucosyltransferase 10; TPM, transcripts per million; ccRCC, clear cell renal cell carcinoma; TCGA, The Cancer Genome Atlas.

breast cancer (37), non-small cell lung cancer (38), prostate cancer (39), and so on. Secondly, it is the AA metabolic process that plays a key role in carcinogenesis, and AA has been considered a novel preventive and therapeutic target in cancer (40,41). For example, AA and metabolic prostaglandin E2 (PGE2) as immune regulators modulate tissue homeostasis and pathological processes in squamous cell carcinoma (42). In hepatocellular carcinoma, berberine elevates the ratio of AA to PGE2 by inhibiting the AA metabolic pathway to induce apoptosis (43). Lastly, PID is correlated with recurrent infections, autoimmunity, and cancers. To our knowledge, there have been numerous previous reports about PID in tumors. It is viewed that the normal and deficient immune system needs to focus on the structure and dynamic function of the immune system as a whole rather than on its isolated components alone (44).

A highlight of this work is the prediction of the effects of *FUT10* on immune infiltration and possible mechanisms in ccRCC cells. Aberrant glycosylation is usually regarded as one of the hallmarks of cancer and is involved in processes from cell signaling pathways, tumor invasion, and immune regulation (10). Co-expression gene analysis suggested that *FUT10* was positively relevant to *ARL8B*, *STAM2*, *APPL1*, *ERLIN2*, *ANKFY1*, *BAG4*, and so on. Those genes play roles in tumor cell proliferation, migration, adhesion, cell cycle and survival, immune response, and so on. Remarkably, *ARL8B*, a related adenosine diphosphate (ADP)-ribosylation factor-like (ARL) family member, has become an important regulator that helps lysosomal transport to the periphery (45). It has also been reported that *ARL8B* may be a key factor in NK-mediated cytotoxicity by transferring polarization of dissolved particles toward immune synapses (46). In addition, we also found an interesting molecule, *STAM2*, which contains a single SH3 domain and an immune receptor tyrosine activation motif (*ITAM*) (47). Meanwhile, *STAM2* has an indispensable role during T cell development and survival, as well as *STAM1* (48).

The immune system plays a vital role in tumor progression. Innate immune cells and adaptive immune cells often reside in the tumor microenvironment and determine the growth rate of tumor (49). RCC is one of the

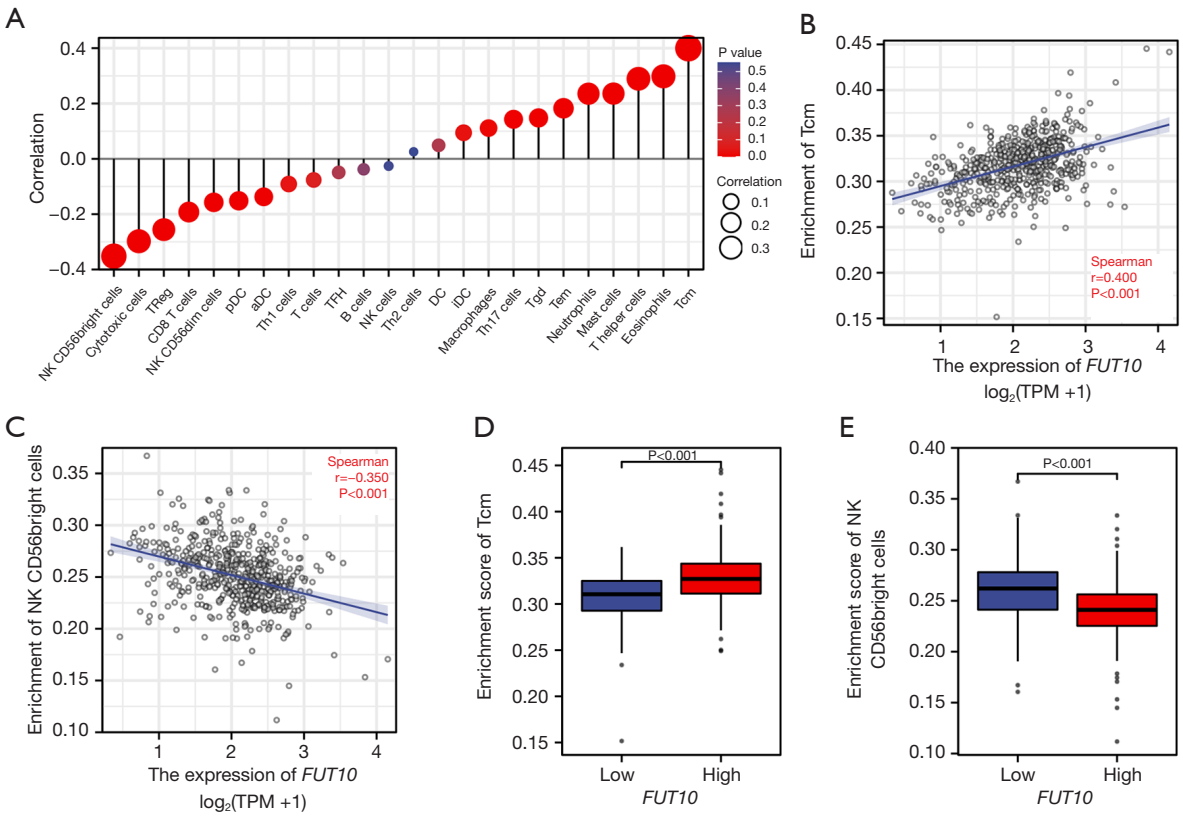

Figure 7 The correlation between *FUT10* expression and immune infiltration in ccRCC based on TCGA data. (A) the association of *FUT10* expression with 24 immune cell types. (B) *FUT10* expression was positively related to Tcm cells. (C) *FUT10* expression was negatively related to NK CD56bright cells. (D) Tcm cells were highly enriched with higher *FUT10* expression. (E) NK CD56bright cells were lowly enriched with higher *FUT10* expression. NK, natural killer; TReg, regulatory T cell; pDC, plasmacytoid dendritic cell; aDC, activated dendritic cell; Th, T helper; TFH, follicular helper T cell; DC, dendritic cell; iDC, immature dendritic cell; Tgd, gamma delta T cell; Tem, effector memory T cell; Tcm, central memory T; *FUT10*, fucosyltransferase 10; TPM, transcripts per million; ccRCC, clear cell renal cell carcinoma; TCGA, The Cancer Genome Atlas.

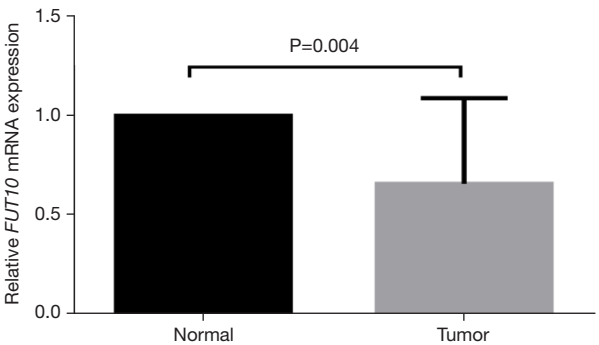

Figure 8 Testified the expression of *FUT10* in adjacent kidney and ccRCC tissues by qRT-PCR (P=0.004). *FUT10*, fucosyltransferase 10; ccRCC, clear cell renal cell carcinoma; qRT-PCR, quantitative real-time polymerase chain reaction.

malignant tumors with the strongest immune infiltration (50-52). Previous studies have shown that activation of specific metabolic pathways can regulate angiogenesis and inflammatory signals (53,54). Tumor microenvironment can affect the response of anti-tumor therapy (35,55-58). *FUT10* can modulate immune cell infiltration and regulate immunoflogosis. We explored whether *FUT10* was related to immune regulation through GO and ssGSEA analysis in ccRCC. Genes related to acute inflammatory response, humoral immune response, regulation of inflammatory response, and lymphocyte-mediated immunity were enriched. In addition, NK CD56bright cells and NK CD56dim cells were negatively correlated with *FUT10* expression, and those were less enriched in the *FUT10*

high expression groups. Thus, *FUT10* may positively regulate NK-mediated immune response by co-expressing with *ARL8B* to affect the progression of ccRCC further. However, this inference still needs further exploration at the cellular level.

An increasing body of literature mainly reports the effect of FUTs 1–8 on various tumors. Our previous research mainly focused on the function and action mechanism of *FUT2* on the proliferation, migration, invasion, apoptosis, and autophagy in lung adenocarcinoma (59-61). Our work is the first exploration of *FUT10* in ccRCC, which is the vanguard in pursuing further biological processing and molecular mechanism research.

Nevertheless, our study still has some limitations. First, our research is based on bioinformatics analysis and lacks comprehensive cell and animal experimental verification, which should be improved in subsequent studies. Second, only PCR experiments were performed, and the lack of independent validation with additional functional wet lab experiments using cell lines or clinical specimens weakens this study. Therefore, in the follow-up study, we will further verify the role and mechanism of FUT in ccRCC at the level of cells, animals, and clinical samples.

Conclusions

In summary, we observed decreasing *FUT10* in ccRCC, which had extraordinary accuracy in the diagnosis and prediction of the primary clinical stage, as well as correlation with the primary clinical stage and correlation with the survival of ccRCC patients. Besides, *FUT10* might participate in the development and progression of ccRCC through multi-signaling pathways and the impact on the immune infiltrating cells, particularly Tcm and NK CD56bright cells. In particular, we found a related molecule of NK-mediated cytotoxicity—*ARL8B*—which may co-express with *FUT10*, but its specific mechanism needs further investigation and clarification. This study revealed the role of *FUT10* in ccRCC and provided a potential biomarker for the diagnosis and prognosis of ccRCC.

Acknowledgments

None.

Footnote

Reporting Checklist: The authors have completed the TRIPOD reporting checklist. Available at https://tcr.amegroups.com/article/view/10.21037/tcr-24-449/rc

Data Sharing Statement: Available at https://tcr.amegroups.com/article/view/10.21037/tcr-24-449/dss

Peer Review File: Available at https://tcr.amegroups.com/article/view/10.21037/tcr-24-449/prf

Funding: None.

Conflicts of Interest: All authors have completed the ICMJE uniform disclosure form (available at https://tcr.amegroups.com/article/view/10.21037/tcr-24-449/coif). The authors have no conflicts of interest to declare.

Ethical Statement: The authors are accountable for all aspects of the work in ensuring that questions related to the accuracy or integrity of any part of the work are appropriately investigated and resolved. The study was conducted in accordance with the Declaration of Helsinki (as revised in 2013).

References

1. Hsieh JJ, Purdue MP, Signoretti S, et al. Renal cell carcinoma. Nat Rev Dis Primers 2017;3:17009.
2. Clark DJ, Dhanasekaran SM, Petralia F, et al. Integrated Proteogenomic Characterization of Clear Cell Renal Cell Carcinoma. Cell 2019;179:964-983.e31.
3. Doppalapudi SK, Leopold ZR, Thaper A, et al. Clearing up Clear Cell: Clarifying the Immuno-Oncology Treatment Landscape for Metastatic Clear Cell RCC. Cancers (Basel) 2021;13:4140.
4. Kim MC, Jin Z, Kolb R, et al. Updates on Immunotherapy and Immune Landscape in Renal Clear Cell Carcinoma. Cancers (Basel) 2021;13:5856.
5. Ljungberg B, Bensalah K, Canfield S, et al. EAU

guidelines on renal cell carcinoma: 2014 update. Eur Urol 2015;67:913-24.
6. Patard JJ, Kim HL, Lam JS, et al. Use of the University of California Los Angeles integrated staging system to predict survival in renal cell carcinoma: an international multicenter study. J Clin Oncol 2004;22:3316-22.
7. Znaor A, Lortet-Tieulent J, Laversanne M, et al. International variations and trends in renal cell carcinoma incidence and mortality. Eur Urol 2015;67:519-30.
8. Lai Y, Tang F, Huang Y, et al. The tumour microenvironment and metabolism in renal cell carcinoma targeted or immune therapy. J Cell Physiol 2021;236:1616-27.
9. Blanas A, Sahasrabudhe NM, Rodríguez E, et al. Fucosylated Antigens in Cancer: An Alliance toward Tumor Progression, Metastasis, and Resistance to Chemotherapy. Front Oncol 2018;8:39.
10. Pinho SS, Reis CA. Glycosylation in cancer: mechanisms and clinical implications. Nat Rev Cancer 2015;15:540-55.
11. Becker DJ, Lowe JB. Fucose: biosynthesis and biological function in mammals. Glycobiology 2003;13:41R-53R.
12. Munkley J, Elliott DJ. Hallmarks of glycosylation in cancer. Oncotarget 2016;7:35478-89.
13. Kumar A, Torii T, Ishino Y, et al. The Lewis X-related α1,3-fucosyltransferase, Fut10, is required for the maintenance of stem cell populations. J Biol Chem 2013;288:28859-68.
14. Shan M, Yang D, Dou H, et al. Fucosylation in cancer biology and its clinical applications. Prog Mol Biol Transl Sci 2019;162:93-119.
15. Vivian J, Rao AA, Nothaft FA, et al. Toil enables reproducible, open source, big biomedical data analyses. Nat Biotechnol 2017;35:314-6.
16. Yu G, Wang LG, Han Y, et al. clusterProfiler: an R package for comparing biological themes among gene clusters. OMICS 2012;16:284-7.
17. Hänzelmann S, Castelo R, Guinney J. GSVA: gene set variation analysis for microarray and RNA-seq data. BMC Bioinformatics 2013;14:7.
18. Bindea G, Mlecnik B, Tosolini M, et al. Spatiotemporal dynamics of intratumoral immune cells reveal the immune landscape in human cancer. Immunity 2013;39:782-95.
19. Gaziel-Sovran A, Segura MF, Di Micco R, et al. miR-30b/30d regulation of GalNAc transferases enhances invasion and immunosuppression during metastasis. Cancer Cell 2011;20:104-18.
20. Bird-Lieberman EL, Neves AA, Lao-Sirieix P, et al. Molecular imaging using fluorescent lectins permits rapid endoscopic identification of dysplasia in Barrett's esophagus. Nat Med 2012;18:315-21.
21. Andergassen U, Liesche F, Kölbl AC, et al. Glycosyltransferases as Markers for Early Tumorigenesis. Biomed Res Int 2015;2015:792672.
22. Meany DL, Chan DW. Aberrant glycosylation associated with enzymes as cancer biomarkers. Clin Proteomics 2011;8:7.
23. Mollicone R, Moore SE, Bovin N, et al. Activity, splice variants, conserved peptide motifs, and phylogeny of two new alpha1,3-fucosyltransferase families (FUT10 and FUT11). J Biol Chem 2009;284:4723-38.
24. di Meo NA, Lasorsa F, Rutigliano M, et al. The dark side of lipid metabolism in prostate and renal carcinoma: novel insights into molecular diagnostic and biomarker discovery. Expert Rev Mol Diagn 2023;23:297-313.
25. Lucarelli G, Loizzo D, Franzin R, et al. Metabolomic insights into pathophysiological mechanisms and biomarker discovery in clear cell renal cell carcinoma. Expert Rev Mol Diagn 2019;19:397-407.
26. di Meo NA, Lasorsa F, Rutigliano M, et al. Renal Cell Carcinoma as a Metabolic Disease: An Update on Main Pathways, Potential Biomarkers, and Therapeutic Targets. Int J Mol Sci 2022;23:14360.
27. De Marco S, Torsello B, Minutiello E, et al. The cross-talk between Abl2 tyrosine kinase and TGFβ1 signalling modulates the invasion of clear cell Renal Cell Carcinoma cells. FEBS Lett 2023;597:1098-113.
28. Bianchi C, Meregalli C, Bombelli S, et al. The glucose and lipid metabolism reprogramming is grade-dependent in clear cell renal cell carcinoma primary cultures and is targetable to modulate cell viability and proliferation. Oncotarget 2017;8:113502-15.
29. Ragone R, Sallustio F, Piccinonna S, et al. Renal Cell Carcinoma: A Study through NMR-Based Metabolomics Combined with Transcriptomics. Diseases 2016;4:7.
30. Lucarelli G, Galleggiante V, Rutigliano M, et al. Metabolomic profile of glycolysis and the pentose phosphate pathway identifies the central role of glucose-6-phosphate dehydrogenase in clear cell-renal cell carcinoma. Oncotarget 2015;6:13371-86.
31. Lucarelli G, Rutigliano M, Sallustio F, et al. Integrated multi-omics characterization reveals a distinctive metabolic signature and the role of NDUFA4L2 in promoting angiogenesis, chemoresistance, and mitochondrial dysfunction in clear cell renal cell carcinoma. Aging (Albany NY) 2018;10:3957-85.
32. Bombelli S, Torsello B, De Marco S, et al. 36-kDa

Annexin A3 Isoform Negatively Modulates Lipid Storage in Clear Cell Renal Cell Carcinoma Cells. Am J Pathol 2020;190:2317-26.
33. Lucarelli G, Rutigliano M, Loizzo D, et al. MUC1 Tissue Expression and Its Soluble Form CA15-3 Identify a Clear Cell Renal Cell Carcinoma with Distinct Metabolic Profile and Poor Clinical Outcome. Int J Mol Sci 2022;23:13968.
34. Milella M, Rutigliano M, Lasorsa F, et al. The Role of MUC1 in Renal Cell Carcinoma. Biomolecules 2024;14:315.
35. Lucarelli G, Netti GS, Rutigliano M, et al. MUC1 Expression Affects the Immunoflogosis in Renal Cell Carcinoma Microenvironment through Complement System Activation and Immune Infiltrate Modulation. Int J Mol Sci 2023;24:4814.
36. Sica V, Bravo-San Pedro JM, Stoll G, et al. Oxidative phosphorylation as a potential therapeutic target for cancer therapy. Int J Cancer 2020;146:10-7.
37. Lee KM, Giltnane JM, Balko JM, et al. MYC and MCL1 Cooperatively Promote Chemotherapy-Resistant Breast Cancer Stem Cells via Regulation of Mitochondrial Oxidative Phosphorylation. Cell Metab 2017;26:633-647.e7.
38. Lissanu Deribe Y, Sun Y, Terranova C, et al. Mutations in the SWI/SNF complex induce a targetable dependence on oxidative phosphorylation in lung cancer. Nat Med 2018;24:1047-57.
39. Farge T, Saland E, de Toni F, et al. Chemotherapy-Resistant Human Acute Myeloid Leukemia Cells Are Not Enriched for Leukemic Stem Cells but Require Oxidative Metabolism. Cancer Discov 2017;7:716-35.
40. Ng CF, Wan SH, Wong A, et al. Use of the University of California Los Angeles Integrated Staging System (UISS) to predict survival in localized renal cell carcinoma in an Asian population. Int Urol Nephrol 2007;39:699-703.
41. Yarla NS, Bishayee A, Sethi G, et al. Targeting arachidonic acid pathway by natural products for cancer prevention and therapy. Semin Cancer Biol 2016;40-41:48-81.
42. Xu M, Wang X, Li Y, et al. Arachidonic Acid Metabolism Controls Macrophage Alternative Activation Through Regulating Oxidative Phosphorylation in PPARγ Dependent Manner. Front Immunol 2021;12:618501.
43. Li J, Li O, Kan M, et al. Berberine induces apoptosis by suppressing the arachidonic acid metabolic pathway in hepatocellular carcinoma. Mol Med Rep 2015;12:4572-7.
44. Haas OA. Primary Immunodeficiency and Cancer Predisposition Revisited: Embedding Two Closely Related Concepts Into an Integrative Conceptual Framework. Front Immunol 2018;9:3136.
45. Bagshaw RD, Callahan JW, Mahuran DJ. The Arf-family protein, Arl8b, is involved in the spatial distribution of lysosomes. Biochem Biophys Res Commun 2006;344:1186-91.
46. Tuli A, Thiery J, James AM, et al. Arf-like GTPase Arl8b regulates lytic granule polarization and natural killer cell-mediated cytotoxicity. Mol Biol Cell 2013;24:3721-35.
47. Endo K, Takeshita T, Kasai H, et al. STAM2, a new member of the STAM family, binding to the Janus kinases. FEBS Lett 2000;477:55-61.
48. Yamada M, Ishii N, Asao H, et al. Signal-transducing adaptor molecules STAM1 and STAM2 are required for T-cell development and survival. Mol Cell Biol 2002;22:8648-58.
49. T G S. Innate and adaptive immune cells in Tumor microenvironment. Gulf J Oncolog 2021;1:77-81.
50. Vuong L, Kotecha RR, Voss MH, et al. Tumor Microenvironment Dynamics in Clear-Cell Renal Cell Carcinoma. Cancer Discov 2019;9:1349-57.
51. Tamma R, Rutigliano M, Lucarelli G, et al. Microvascular density, macrophages, and mast cells in human clear cell renal carcinoma with and without bevacizumab treatment. Urol Oncol 2019;37:355.e11-9.
52. Gigante M, Pontrelli P, Herr W, et al. miR-29b and miR-198 overexpression in CD8+ T cells of renal cell carcinoma patients down-modulates JAK3 and MCL-1 leading to immune dysfunction. J Transl Med 2016;14:84.
53. Netti GS, Lucarelli G, Spadaccino F, et al. PTX3 modulates the immunoflogosis in tumor microenvironment and is a prognostic factor for patients with clear cell renal cell carcinoma. Aging (Albany NY) 2020;12:7585-602.
54. Lucarelli G, Rutigliano M, Ferro M, et al. Activation of the kynurenine pathway predicts poor outcome in patients with clear cell renal cell carcinoma. Urol Oncol 2017;35:461.e15-27.
55. Lasorsa F, Rutigliano M, Milella M, et al. Complement System and the Kidney: Its Role in Renal Diseases, Kidney Transplantation and Renal Cell Carcinoma. Int J Mol Sci 2023;24:16515.
56. Lasorsa F, di Meo NA, Rutigliano M, et al. Immune Checkpoint Inhibitors in Renal Cell Carcinoma: Molecular Basis and Rationale for Their Use in Clinical Practice. Biomedicines 2023;11:1071.
57. Ghini V, Laera L, Fantechi B, et al. Metabolomics to Assess Response to Immune Checkpoint Inhibitors in Patients with Non-Small-Cell Lung Cancer. Cancers (Basel) 2020;12:3574.

58. Lasorsa F, Rutigliano M, Milella M, et al. Cellular and Molecular Players in the Tumor Microenvironment of Renal Cell Carcinoma. J Clin Med 2023;12:3888.
59. Zhou W, Ma H, Deng G, et al. Clinical significance and biological function of fucosyltransferase 2 in lung adenocarcinoma. Oncotarget 2017;8:97246-59.
60. Deng G, Chen L, Zhang Y, et al. Fucosyltransferase 2 induced epithelial-mesenchymal transition via TGF-β/Smad signaling pathway in lung adenocarcinaoma. Exp Cell Res 2018;370:613-22.
61. Zhang Y, Yao E, Liu Y, et al. FUT2 Facilitates Autophagy and Suppresses Apoptosis via p53 and JNK Signaling in Lung Adenocarcinoma Cells. Cells 2022;11:4031.

Cite this article as: Zhang Y, Cui K, Qiang R, Wang L. *FUT10* is related to the poor prognosis and immune infiltration in clear cell renal cell carcinoma. Transl Cancer Res 2025;14(2):827-842. doi: 10.21037/tcr-24-449